Phase transition patterns in relativistic and nonrelativistic multi-scalar-field models

Marcus Benghi Pinto,[1,*] Rudnei O. Ramos,[2,†] and Júlia E. Parreira[1,‡]

[1]*Departamento de Física, Universidade Federal de Santa Catarina, 88040-900 Florianópolis, Santa Catarina, Brazil*
[2]*Departamento de Física Teórica, Universidade do Estado do Rio de Janeiro, 20550-013 Rio de Janeiro, RJ, Brazil*

We discuss the phenomena of symmetry nonrestoration and inverse symmetry breaking in the context of multi-scalar field theories at finite temperatures and present its consequences for the relativistic Higgs-Kibble multi-field sector as well as for a nonrelativistic model of hard core spheres. For relativistic scalar field models, it has been shown previously that temperature effects on the couplings do not alter, qualitatively, the phase transition pattern. Here, we show that for the nonrelativistic analogue of these models inverse symmetry breaking, as well as symmetry nonrestoration, cannot take place, at high temperatures, when the temperature dependence of the two-body couplings is considered. However, the temperature behavior in the nonrelativistic models allows for the appearance of reentrant phases.

I. INTRODUCTION

The study of symmetry breaking (SB) and symmetry restoration (SR) mechanisms have proved to be extremely useful in the analysis of phenomena related to phase transitions in almost all branches of physics. Some topics of current interest which make extensive use of SB/SR mechanisms are topological defects formation in cosmology, the Higgs-Kibble mechanism in the standard model of elementary particles and the Bose-Einstein condensation (BEC) in condensed matter physics. An almost general rule that arises from those studies is that a symmetry which is broken at zero temperature should get restored as the temperature increases. Examples range from the traditional ferromagnet to the more up to date chiral symmetry breaking/restoration in QCD, with the transition pattern being the simplest one of going from the broken phase to the symmetric one as temperature goes from below to above some critical value and vice-versa.

However, a counter-intuitive example may happen in multifield models, as first noticed by Weinberg [1] who considered an $O(N_\phi) \times O(N_\psi)$ invariant relativistic model with two types of scalar fields (with N_ϕ and N_ψ components) and different types of self and crossed interactions. Using the one-loop approximation he has shown that it is possible for the crossed coupling constant to be negative, while the model is still bounded from below, leading, for some parameter values, to an enhanced symmetry breaking effect at high temperatures. This would predict that a symmetry which is broken at $T = 0$ may not get restored at high temperatures, a phenomenon known as symmetry nonrestoration (SNR), or, in the opposite case, a symmetry that is unbroken at $T = 0$ would become broken at high temperatures, thus characterizing inverse symmetry breaking (ISB). Here, one could argue that SNR/ISB are perhaps just artifacts of the simple one-loop perturbative approximation and that the consideration of higher order terms and effects like the temperature dependence of the couplings could change the situation. To answer this question the model has been reinvestigated by many other authors using a variety of different methods with most results giving further support to the idea (see, e.g., Ref. [2] for a short review of SNR/ISB). For example, the SNR/ISB phenomena were studied using the Wilson Renormalization Group [3] and the explicit running of the (temperature dependent) coupling constants has been taken into account, showing that in fact the strength of all couplings increases in approximately the same way with the temperature. This analysis shows that once the couplings are set, at some (temperature) scale, such as to make SNR/ISB possible, the situation cannot be reversed at higher temperatures. Two of the present authors have also treated the problem nonperturbatively taking full account of the cumbersome two-loop contributions [4]. The results obtained in Ref. [4] were shown to be in good agreement with those obtained using the renormalization group approach of Ref. [3] and, therefore, also support the possibility of SNR/ISB occurring in relativistic multiscalar field models even at extremely high temperatures, where standard perturbation theory would break down.

The mechanisms of SNR/ISB have found a variety of applications. For instance, in cosmology, where they have been implemented in realistic models, their consequences have been explored in connection with high temperature phase transitions in the early Universe, with applications covering problems involving *CP* violation and baryogenesis, topological defect formation, inflation, etc. [5,6]. For example, the Kibble-Higgs sector of a $SU(5)$ grand unified theory can be mimicked by considering the case $N_\phi = 90$ and $N_\psi = 24$ and has been used to treat the monopole problem [5–7]. Setting $N_\phi = N_\psi = 1$ the model becomes invariant under the discrete transformation $Z_2 \times Z_2$. The latter version has been used in connection with the domain wall problem [8]. Most applications are listed in Ref. [2]

*Electronic address: marcus@fsc.ufsc.br
†Electronic address: rudnei@uerj.br
‡Electronic address: juliaep@fsc.ufsc.br

which gives an introduction to the subject discussing other contexts in which SNR/ISB can take place in connection with cosmology and condensed matter physics. These interesting results from finite temperature quantum field theory raise important questions regarding their possible manifestation in condensed matter systems which can be described by means of *nonrelativistic* scalar field theories in the framework of the phenomenology of Ginzburg-Landau potentials, like, for example, in homogeneous Bose gases [9]. As far as these systems are concerned, we are unaware of any applications or studies of analogue SNR/ISB phenomena in the context of nonrelativistic scalar field models.

In the context of condensed matter physics more exotic transitions are well known to be possible and similar phenomena to ISB/SNR have been observed in a large variety of materials. One of the best known examples is the symmetry pattern observed in potassium sodium tartrate tetrahydrate, $KNa(C_4H_4O_6).4H_2O$, most commonly known as the Rochelle salt, which goes [10], as the temperature increases, from a more symmetric orthorhombic crystalline structure to a less symmetric monoclinic structure at $T \simeq 255K$. It then returns to be orthorhombic phase at $T \simeq 297K$, till it melts at $T \simeq 348K$. It thus exhibits an intermediary inverse symmetry breaking-like phenomenon through a reentrant phase. Other materials which arose great interest recently due to their potential applications include, for example, the liquid crystals [11] and spin glass materials [12], which exhibit analogous phenomena of having less symmetric phases at intermediary temperature ranges, known as nematic to smectic phases (ferro and antiferro electric and magnetic like phases), and compounds known as the manganites, e.g. $(Pr, Ca, Sr)MnO_3$, which can exhibit ferromagnetic like reentrant phases above the Curie (critical) temperature [13]. Actually, in the condensed matter literature we can find many other examples of physical materials exhibiting analogue phenomena of SNR/ISB. This same trend of the emergence of reentrant phases also seems to include low dimensional systems [14]. A discussion on these inverse like symmetry breaking phenomena in condensed matter systems has been recently summarized in Ref. [15]. Another motivation for the present work is the growing interest in investigating parallels between symmetry breaking in particle physics (Cosmology) and condensed matter physics (the Laboratory) as discussed by Rivers [16] in a recent review related to the COSLAB programme. One of the most exciting aspects of such investigation is due to the fact that condensed matter allows for experiments which can, in principle, test models and/or methods used in Cosmology.

Here, our aim is to analyze a nonrelativistic model composed of two different types of multicomponent fields. To investigate SNR/ISB we consider a model possessing an $U(1) \times U(1)$ global symmetry, that is analogous to the $O(N_\phi) \times O(N_\psi)$ relativistic model studied in [1,3,4], for $N_\phi = N_\psi = 2$, including both one and two-body interactions in the potential. Further, by disregarding the bosonic internal degrees of freedom, the model is considered as representing a system of hard core spheres. In the analysis that follows in the next sections we do not claim that this simplified model described in terms of scalar fields with local interactions will be simulating the phases behavior of any of the condensed matter system cited in the previous paragraph, but just that it suffices, as a toy model, to show the generality of the possibility of emergence of reentrant behavior in some simple condensed matter systems which can be modeled by coupled multiscalar field models. The chosen nonrelativistic model is also simple enough to show the differences and analogies regarding the phenomena of SNR/ISB which occurs on its relativistic counterpart.

We will show that, like in the relativistic case, SNR/ISB can take place when thermal effects on the couplings are neglected. We then consider these thermal effects by computing the first one-loop contributions to the couplings finding that, contrary to the relativistic case, SNR/ISB cannot persist indefinitely at higher temperatures when all symmetries are restored. In summary, the possible phase transition patterns seem to be completely different for the relativistic and nonrelativistic cases when the important thermal effects on the couplings are taken into account. This paper is divided as follows. In Sec. II we review the original relativistic prototype model. In Sec. III we present a similar nonrelativistic model of hard core spheres with quadratic and quartic interactions. We show how SNR/ISB cannot occur for such a system when the temperature effects on the couplings are considered, but they can only manifest through reentrant like phases, with symmetry restoration always happening at high enough temperatures. Our conclusions and final remarks are presented in Sec. IV. An appendix is included to show some technical details of the calculations.

II. THE EMERGENCE OF SNR/ISB PHENOMENA IN THE RELATIVISTIC MODEL

At finite temperature the relativistic multiscalar field theory was first studied by Weinberg [1] who found evidence of SNR/ISB taking place at finite temperatures. On his work, he considered a prototype model composed of two types of scalar fields, ϕ and ψ with N_ϕ and N_ψ components, respectively, which is invariant under the $O(N_\phi) \times O(N_\psi)$ transformation. Such a model has a Lagrangian density which can then be written as

$$\mathcal{L}(\phi, \psi) = \frac{1}{2}(\partial_\mu \phi)^2 - \frac{m_\phi^2}{2}\phi^2 - \frac{\lambda_\phi}{4!}(\phi^2)^2 + \frac{1}{2}(\partial_\mu \psi)^2$$
$$- \frac{m_\psi^2}{2}\psi^2 - \frac{\lambda_\psi}{4!}(\psi^2)^2 - \frac{\lambda}{4}\phi^2\psi^2. \quad (2.1)$$

The self-coupling constants λ_ϕ and λ_ψ and the cross-coupling λ in Eq. (2.1) are traditionally considered as all

positive. However, it is still possible to consider λ negative in (2.1) provided the potential is kept bounded from below. It is easily seen in this case that the boundness condition for the model (2.1) requires that the couplings satisfy

$$\lambda_\phi > 0, \qquad \lambda_\psi > 0, \qquad \lambda_\phi \lambda_\psi > 9\lambda^2. \qquad (2.2)$$

The fact that the cross-coupling, λ, is allowed to be negative has interesting consequences as is seen from the one-loop thermal mass evaluation. As usual, the temperature effects on the zero temperature mass parameters m_i^2 (where $i = \phi$ or ψ) can be computed from the (thermal) self-energy corrections $\Sigma_i(T)$ from which the thermal masses, $M_i^2(T) = m_i^2(0) + \Sigma_i(T)$ are obtained. The thermal masses have been first calculated with the one-loop approximation [1] which, using the usual rules of finite temperature quantum field theory (see e.g. [1,17]) and in the high temperature approximation, $m_\phi/T, m_\psi/T \ll 1$, leads to the results

$$M_\phi^2(T) \simeq m_\phi^2 + \frac{T^2}{12}\left[\lambda_\phi \frac{1}{2}\left(\frac{N_\phi + 2}{3}\right) + \lambda \frac{N_\psi}{2}\right], \qquad (2.3)$$

and

$$M_\psi^2(T) \simeq m_\psi^2 + \frac{T^2}{12}\left[\lambda_\psi \frac{1}{2}\left(\frac{N_\psi + 2}{3}\right) + \lambda \frac{N_\phi}{2}\right], \qquad (2.4)$$

where we kept only the leading order relevant thermal contributions in the high temperature expansion of $\Sigma_i(T)$, which will be enough for the analysis that follows. Note also that the zero temperature quantum corrections to both masses and coupling constants are divergent quantities and so require renormalization. This is done the standard way by adding the appropriate counterterms of renormalization in (2.1) (see also [4]). We are only interested in the thermal quantities (that are finite) since the zero temperature quantum corrections to masses and couplings can be regarded as negligible as compared to the finite temperature contributions. In Eqs. (2.3) and (2.4), as well as in the relations below, the mass parameters m_ϕ and m_ψ and couplings λ_ϕ, λ_ϕ and λ are just to be interpreted here as the renormalized quantities instead of the bare ones. It is obvious, from the potential term in the Lagrangian density (2.1), that if one of the mass parameters m_i^2 is negative the $O(N_i)$ symmetry related to that sector is broken at $T = 0$: $O(N_i) \rightarrow O(N_i - 1)$. Thermal effects tend to restore that symmetry at a certain critical temperature, upon using Eqs. (2.3) and (2.4), given by

$$T_{c,i} = \left\{-12m_i^2\left[\lambda_i \frac{1}{2}\left(\frac{N_i + 2}{3}\right) + \lambda \frac{N_j}{2}\right]^{-1}\right\}^{1/2}. \qquad (2.5)$$

However, if $m_i^2 < 0$, Eq. (2.5) shows that for a negative cross-coupling constant, $\lambda < 0$, and for $|\lambda| > \lambda_i(N_i + 2)/(3N_j)$, $T_{c,i}$ cannot be real. In other words, the broken symmetry is never restored (SNR). At the same time if $m_i^2 > 0$ (unbroken $O(N_i)$ symmetry at $T = 0$) but $\lambda < 0$

and $|\lambda| > \lambda_i(N_i + 2)/(3N_j)$ then from Eqs. (2.3), (2.4), and (2.5), we can predict that, as the temperature is increased, the symmetry will be broken at T_c, instead of being restored (ISB). For example, let us suppose that $\lambda < 0$ and

$$|\lambda| > \frac{\lambda_\phi}{N_\psi}\left(\frac{N_\phi + 2}{3}\right). \qquad (2.6)$$

In this case the boundness condition assures that $|\lambda| < \lambda_\psi(N_\psi + 2)/(3N_\phi)$. Then, if $m_\psi^2 < 0$ one has broken $O(N_\phi)$ symmetry at $T = 0$, but $M_\psi^2(T)$ will eventually become positive at the corresponding $T_{c,\psi}$, given by Eq. (2.5), restoring the symmetry. If $m_\psi^2 > 0$, then $M_\psi^2(T) > 0$ for all values of T and the model is always symmetric under $O(N_\psi)$. On the other hand, if $m_\phi^2 < 0$, our choice of parameters predicts that the $O(N_\phi)$ symmetry is broken at $T = 0$ and that it does not get restored at high temperatures, a clear manifestation of SNR. At the same time, if $m_\phi^2 > 0$, the $O(N_\phi)$ symmetry, which is unbroken at $T = 0$, becomes broken at a $T \geq T_{c,\phi}$, which is a manifestation of ISB. Obviously, which field will suffer SNR or ISB depends on our initial arbitrary choice of parameter values. Note that when $\lambda = 0$ the theory decouples and SNR/ISB cannot take place. In this case one observes the usual SR which happens in the simple $O(N)$ scalar model.

An issue that arises, concerning the results discussed above, is that the coupling constants are scale dependent in accordance with the renormalization group equations. Therefore, at high temperatures not only the masses get dressed by thermal corrections but also the coupling constants, so we must answer whether the intriguing phase transitions patterns discussed above, for $\lambda < 0$, can hold in terms of the equivalent running coupling constants. This issue was analyzed by Roos [3], who used the Wilson Renormalization Group (WRG) to evaluate the $\lambda_i(T)$ and $\lambda(T)$. His calculations revealed that the strength of all couplings increase, at high T, in a way which excludes the possibility of SR in cases where SNR/ISB happen. He also showed that the running of coupling constants with temperature as predicted by the one-loop approximation, as adopted in the present work, is robust up to very large scales. In addition to that, the two-loop nonperturbative calculations performed in Ref. [4] also support, from a qualitative point of view, Weinberg's one-loop results.

As one notices from the equations which describe the thermal masses, Eqs. (2.3) and (2.4), the appearance of SNR/ISB is directly related to the relation among the different couplings when $\lambda < 0$. It is then useful to define the quantity

$$\Delta_i = \lambda_i \frac{1}{2}\left(\frac{N_i + 2}{3}\right) + \lambda \frac{N_j}{2}, \qquad (2.7)$$

which takes those relations into account. Then, in terms of temperature independent couplings, the critical tempera-
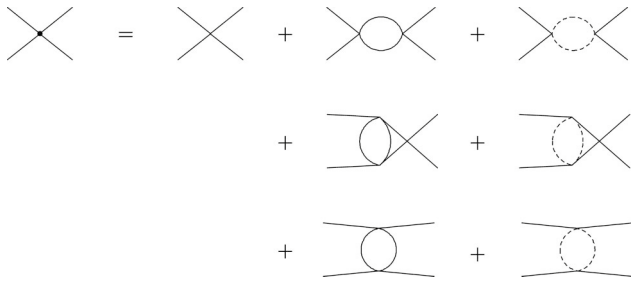
FIG. 1. The diagrammatic representation for the effective coupling $\lambda_\phi(T)$ up to the one-loop level. The continuous lines stand for the ϕ propagators, while the dashed lines represent ψ.

ture, Eq. (2.5), can be written as

$$T_{c,i} = \left(\frac{-12M_i^2}{\Delta_i}\right)^{1/2}. \qquad (2.8)$$

One can easily see that SNR/ISB may occur when *one*[1] of the Δ_i is negative.

Let us now check the robustness of SNR/ISB when the effective, temperature dependent couplings are considered. The thermal effects on all the three couplings, at the one-loop order, are considered in terms of the corrections to the four-point 1PI Green's functions. All diagrams at the one-loop level contributing to the effective couplings $\lambda_\phi(T)$, $\lambda_\psi(T)$ and $\lambda(T)$ are shown in Figs. 1–3, respectively. These diagrams, with zero external momenta,[2] are easily computed at finite temperature (see for instance Refs. [3,18]). Using again the high temperature approximation at leading order, one obtains

$$\lambda_\phi(T) \simeq \lambda_\phi + \frac{3}{8\pi^2} \ln\left(\frac{T}{M_0}\right)\left[\frac{1}{2}\left(\frac{N_\phi + 8}{9}\right)\lambda_\phi^2 + \frac{N_\psi}{2}\lambda^2\right], \qquad (2.9)$$

$$\lambda_\psi(T) \simeq \lambda_\psi + \frac{3}{8\pi^2} \ln\left(\frac{T}{M_0}\right)\left[\frac{1}{2}\left(\frac{N_\psi + 8}{9}\right)\lambda_\psi^2 + \frac{N_\phi}{2}\lambda^2\right], \qquad (2.10)$$

and

$$\lambda(T) \simeq \lambda + \frac{\lambda}{8\pi^2} \ln\left(\frac{T}{M_0}\right)\left[\frac{1}{2}\left(\frac{N_\phi + 2}{3}\right)\lambda_\phi \right.$$
$$\left. + \frac{1}{2}\left(\frac{N_\psi + 2}{3}\right)\lambda_\psi\right] + \frac{\lambda^2}{4\pi^2} \ln\left(\frac{T}{M_0}\right), \qquad (2.11)$$

where M_0 is a regularization scale. In writing the above equations we are once again assuming that the tree-level

---

[1]One of the main results of Ref. [4] states that SNR/ISB can occur in both sectors, for some parameter values, a situation which is not allowed at the one-loop level.

[2]Recall that those are contributions to the effective potential, which generates all 1PI Green's function with zero external momenta.
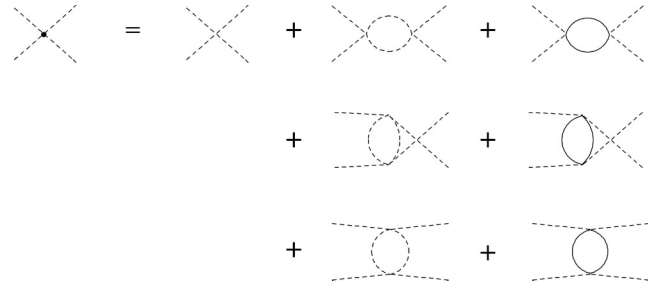
couplings in Eqs. (2.9), (2.10), and (2.11) are the renormalized ones and we also are only showing the relevant high temperature corrections. The same expressions were also obtained by Roos in [3] (note however that different normalizations for the tree-level potential as well as $M_0 = T_0, N_\phi = N_\psi = 1$ were used in that reference). In [3], the numerical solution of the one-loop Wilson renormalization group equations was also compared to the usual flow equations for the constants obtained from the one-loop

FIG. 2. The diagrammatic representation for the effective coupling $\lambda_\psi(T)$ up to the one-loop level.
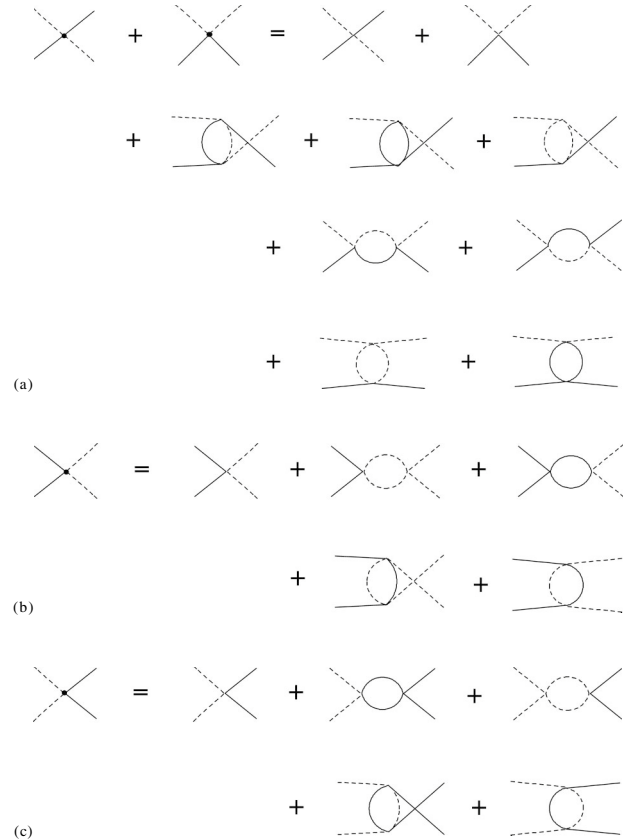

FIG. 3. Diagrams contributing up to the one-loop level to the effective cross-coupling $\lambda(T)$. For convenience we have identified the processes: (a) $\phi\psi \to \phi\psi$, (b) $\phi\phi \to \psi\psi$ and (c) $\psi\psi \to \phi\phi$.

beta-functions and shown to agree well with each other up to very high scales. The flow equations referring to the perturbative effective coupling constants Eqs. (2.9), (2.10), and (2.11) are expressed in term of the dimensionless scale T/M_0 [18] as

$$\frac{d\lambda_\phi(t)}{dt} = \frac{3}{8\pi^2}\left[\frac{1}{2}\left(\frac{N_\phi + 8}{9}\right)\lambda_\phi^2(t) + \frac{N_\psi}{2}\lambda^2(t)\right], \quad (2.12)$$

$$\frac{d\lambda_\psi(t)}{dt} = \frac{3}{8\pi^2}\left[\frac{1}{2}\left(\frac{N_\psi + 8}{9}\right)\lambda_\psi^2(t) + \frac{N_\phi}{2}\lambda^2(t)\right], \quad (2.13)$$

and

$$\frac{d\lambda(t)}{dt} = \frac{\lambda(t)}{8\pi^2}\left[\frac{1}{2}\left(\frac{N_\phi + 2}{3}\right)\lambda_\phi(t) + \frac{1}{2}\left(\frac{N_\psi + 2}{3}\right)\lambda_\psi(t)\right] + \frac{\lambda^2(t)}{4\pi^2}, \quad (2.14)$$

where $t = \ln(T/M_0)$ was used. The solutions of the flow Eqs. (2.12), (2.13), and (2.14), with initial conditions given by the renormalized tree-level coupling constants, can also be easily seen to be equivalent to the solutions for the set of linear coupled equations,

$$\begin{aligned}
\lambda_\phi(T) &= \lambda_\phi + \frac{3}{8\pi^2}\ln\left(\frac{T}{M_0}\right)\left[\frac{1}{2}\left(\frac{N_\phi + 8}{9}\right)\lambda_\phi\lambda_\phi(T) + \frac{N_\psi}{2}\lambda\lambda(T)\right]\lambda_\psi(T) \\
&= \lambda_\psi + \frac{3}{8\pi^2}\ln\left(\frac{T}{M_0}\right)\left[\frac{1}{2}\left(\frac{N_\psi + 8}{9}\right)\lambda_\psi\lambda_\psi(T) + \frac{N_\phi}{2}\lambda\lambda(T)\right]\lambda(T) \\
&= \lambda + \frac{\lambda}{16\pi^2}\ln\left(\frac{T}{M_0}\right)\left[\frac{1}{2}\left(\frac{N_\phi + 2}{3}\right)\lambda_\phi(T) + \frac{1}{2}\left(\frac{N_\psi + 2}{3}\right)\lambda_\psi(T)\right] \\
&\quad + \frac{\lambda(T)}{16\pi^2}\ln\left(\frac{T}{M_0}\right)\left[\frac{1}{2}\left(\frac{N_\phi + 2}{3}\right)\lambda_\phi + \frac{1}{2}\left(\frac{N_\psi + 2}{3}\right)\lambda_\psi\right] + \frac{1}{4\pi^2}\ln\left(\frac{T}{M_0}\right)\lambda\lambda(T). \quad (2.15)
\end{aligned}$$

The results obtained from the flow equations given above, or equivalently from the solutions of coupled set of Eqs. (2.15), are standard ways of nonperturbatively resumming the leading order corrections (in this case the leading log temperature dependent corrections) to the coupling constants. For instance, Eq. (2.15) is exactly the analogous procedure used for the one-field case for summing all ladder (1-loop or bubble) contributions to the effective coupling constant. For the multifield case, the perturbative approximation for (2.15) is again given by Eqs. (2.9), (2.10), and (2.11), at the one-loop level. In our case, these equations are useful to test how robust is the phenomena of SNR/ISB and will be used below in our analysis. Later, in the next section for the nonrelativistic limit of Eq. (2.1), we will also construct the analogous of these nonperturbative equations for the temperature dependent effective couplings.

In terms of the effective temperature dependent couplings, $\lambda_\phi(T)$, $\lambda_\psi(T)$ and $\lambda(T)$ the quantity analogous to Eq. (2.7) becomes

$$\Delta_i(T) = \lambda_i(T)\frac{1}{2}\left(\frac{N_i + 2}{3}\right) + \lambda(T)\frac{N_j}{2}, \quad (2.16)$$

or, more explicitly, using Eqs. (2.9), (2.10), and (2.11),

$$\begin{aligned}
\Delta_i(T) = \lambda_i\left(\frac{N_i + 2}{6}\right) &+ \lambda\frac{N_j}{2} + \lambda_i^2\frac{(N_i + 8)(N_i + 2)}{288\pi^2}\ln\left(\frac{T}{M_0}\right) \\
&+ \lambda N_j\frac{(N_i + 2)\lambda_i + (N_j + 2)\lambda_j}{96\pi^2}\ln\left(\frac{T}{M_0}\right) \\
&+ \lambda^2\frac{N_j(N_i + 6)}{32\pi^2}\ln\left(\frac{T}{M_0}\right). \quad (2.17)
\end{aligned}$$

It is clear from the expressions for the effective couplings,

Eqs. (2.9), (2.10), (2.11), and (2.17), that for perturbative values for the tree-level coupling parameters the predicted results for SNR/ISB are very stable even for very large temperatures (in units of the regularization scale M_0) which is due to the slow logarithmic change with the temperature. As an illustration, consider, for example, the tree-level coupling parameters that satisfy the boundness condition Eq. (2.2), $\lambda_\phi = 7 \times 10^{-5}$, $\lambda_\psi = 5 \times 10^{-4}$ and $\lambda = -6 \times 10^{-5}$ and $N_\phi = N_\psi = 2$. For these values of
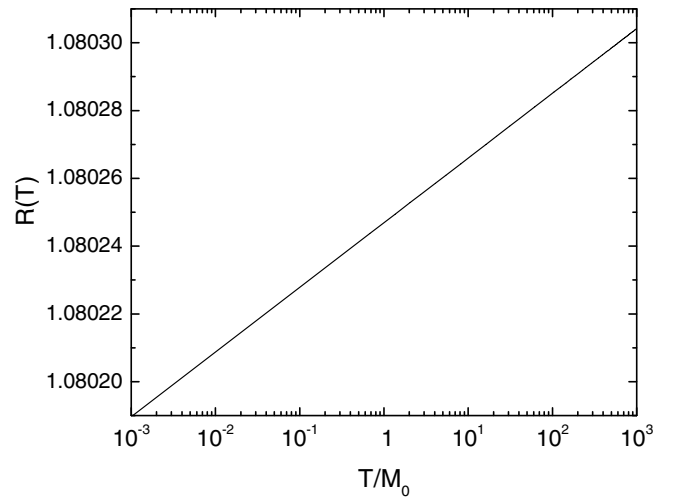

FIG. 4. The boundness condition, Eq. (2.2), expressed in terms of the effective couplings, is shown in the vertical axis as the ratio $R(T) = \lambda_\phi(T)\lambda_\psi(T)/[3\lambda(T)]^2$. The temperature is shown in units of the regularization scale M_0 while $N_\phi = N_\psi = 2$. The tree-level values $\lambda_\phi = 7 \times 10^{-5}$, $\lambda_\psi = 5 \times 10^{-4}$ and $\lambda = -6 \times 10^{-5}$ were considered.
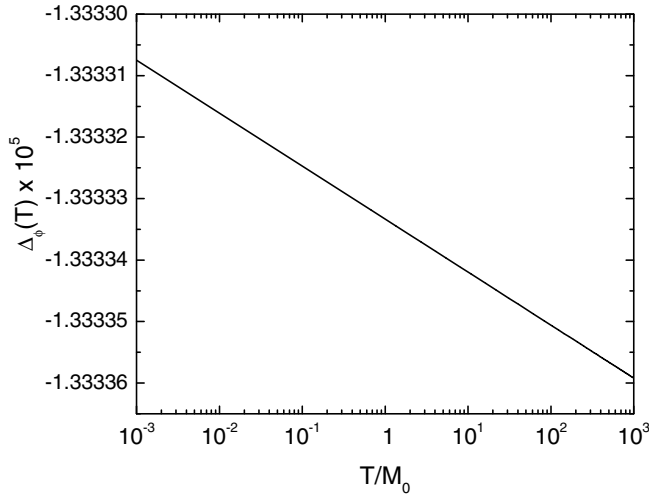
FIG. 5.   The quantity $\Delta_\phi(T)$ as a function of the temperature for the same values of parameters considered in Fig. 4.

parameters Eq. (2.6) is satisfied and the one-loop equations for the effective masses predict ISB or SNR, along the ϕ direction, for $m_\phi^2 > 0$ or $m_\phi^2 < 0$, respectively. Figure 4 shows that the boundness condition also holds true for the effective temperature dependent couplings. Figure 5 shows the quantity $\Delta_\phi(T)$, defined by Eq. (2.16), which remains negative for the whole range of temperatures considered, thus predicting SNR/ISB along the ϕ direction, in accordance with the WRG results [3]. At the same time, $\Delta_\psi(T)$, shown in Fig. 6, remains always positive.

Note that the apparent almost constancy in a wide range of temperatures seen from the Figs. 4–6, is only a consequence of the effective couplings be only logarithmically dependent on T and the very small values for the tree-level couplings that we have considered. Had we taken larger
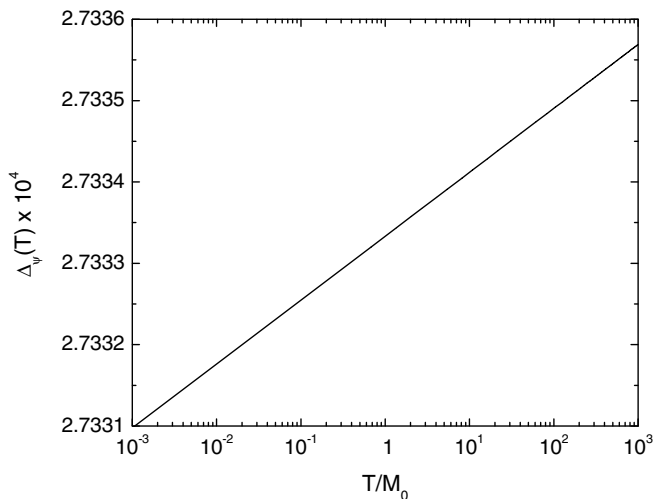

FIG. 6.   The quantity $\Delta_\psi(T)$ as a function of the temperature for the same values of parameters considered in Fig. 4.

values for the tree-level couplings, obviously would lead to a much larger variation with increasing temperature.

Given the results shown above for the relativistic case, we can conclude, therefore, that the inclusion of thermal effects on the couplings does not exclude the possibility of SNR/ISB occurring at high temperatures. We recall that although the results were obtained with the one-loop approximation this feature does not seem to be an artifact of perturbation theory as confirmed by the results produced by nonperturbative methods, such as the Wilson Renormalization Group procedure used in Ref. [3], as well as the optimized perturbation theory used in Ref. [4], where not only thermal corrections to the couplings are accounted for but also to the masses (like in the Schwinger-Dyson or gap equations for the masses).

III. SEARCHING FOR SNR/ISB PATTERNS IN THE NON-RELATIVISTIC CASE

We now turn our attention to the analysis of similar SNR/ISB phenomena displayed by the relativistic model, given by the Lagrangian density, Eq. (2.1), in the case of its nonrelativistic counterpart. Let us first recall some fundamental differences between relativistic and nonrelativistic theories that will be important in our analysis. First, the obvious reduction from Lorentz to Galilean invariance. Second, it should be noted that in the nonrelativistic description particle number is conserved and so, only complex fields are allowed. This second point will be particularly important to us since, for the processes entering in the effective couplings shown in Figs. 1–3, only those that do not change particle number (the elastic processes) will be allowed (e.g. this selects the processes (a) shown in Fig. 3 but not the (b) and (c), inelastic, ones). Another important difference between relativistic and nonrelativistic models concerns the structure of the respective propagators. While the relativistic propagator allows for both forward and backward particle propagation (which is associated to particles and antiparticles, respectively), the nonrelativistic propagator of scalar theories at $T = 0$ only has forward propagation (see e.g. the discussion in Ref. [19]). Note however that the structure of the propagators (or two-point Green's function) in a thermal bath includes both backward and forward propagation [20], which can be interpreted in terms of excitations to and from the thermal bath (or, equivalently, emission and absorption of particle to and from the thermal bath [21]).

We should also say that, alternatively to the derivation of the nonrelativistic analog of (2.1), we could as well consider the relevant equations leading e.g. to the derived effective couplings in the previous section and take the appropriate low-energy limit for those equations. However it is more practical, and indeed it is the procedure usually adopted in atomic and low-energy nuclear physics, to start directly from the nonrelativistic Hamiltonian or Lagrangian densities. This is a one step procedure leading,

say, to the Feynman rules that can be applied to any other quantity that we may be interested in computing, without having first to compute the corresponding relativistic expressions and then working out the corresponding non-relativistic. So, let us now initially consider the nonrelativistic limit of the Lagrangian density given by Eq. (2.1). This can be obtained by first expressing the fields ϕ and ψ in terms of (complex) nonrelativistic fields Φ and Ψ as [19,22,23]

$$\phi(\vec{x}, t) = \frac{1}{\sqrt{2m_\phi}}[\exp(-im_\phi t)\Phi(\vec{x}, t)$$
$$+ \exp(im_\phi t)\Phi^*(\vec{x}, t)], \qquad (3.1)$$

and

$$\psi(\vec{x}, t) = \frac{1}{\sqrt{2m_\psi}}[\exp(-im_\psi t)\Psi(\vec{x}, t)$$
$$+ \exp(im_\psi t)\Psi^*(\vec{x}, t)], \qquad (3.2)$$

where it is assumed that the fields Φ and Ψ oscillate in time much more slowly than $\exp(im_\phi t)$ and $\exp(im_\psi t)$, respectively. By substituting (3.1) and (3.2) in (2.1) and taking the nonrelativistic limit of large masses, the oscillatory terms with frequencies m_ϕ and m_ψ can be dropped. The resulting Lagrangian density in terms of Φ, Ψ and complex conjugate fields becomes

$$\mathcal{L}(\Phi^*, \Phi, \Psi^*, \Psi) = \frac{1}{2m_\phi}[-im_\phi(\partial_t\Phi^*)\Phi + im_\phi\Phi^*(\partial_t\Phi) - |\nabla\Phi|^2 + |\partial_t\Phi|^2] - \frac{\lambda_\phi}{16m_\phi^2}(\Phi^*\Phi)^2 + \frac{1}{2m_\phi}[-im_\psi(\partial_t\Psi^*)\Psi$$
$$+ im_\psi\Psi^*(\partial_t\Psi) - |\nabla\Psi|^2 + |\partial_t\Psi|^2] - \frac{\lambda_\psi}{16m_\psi^2}(\Psi^*\Psi)^2 - \frac{\lambda}{4m_\phi m_\psi}(\Phi^*\Phi)(\Psi^*\Psi), \qquad (3.3)$$

where we have assumed for simplicity, in the derivation of the last term in (3.3), the cross-fields interaction term, that $m_\phi \neq m_\psi$.[3] By further considering

$$|\partial_t\Phi|^2 \ll 2m_\phi\text{Im}(\Phi\partial_t\Phi^*),$$
$$|\partial_t\Psi|^2 \ll 2m_\psi\text{Im}(\Psi\partial_t\Phi^*), \qquad (3.4)$$

we can omit the terms with two time derivatives in Eq. (3.3). So the Lorentz invariance in (3.3) is lost and the nonrelativistic analogue of (2.1) is obtained. The interaction terms in Eq. (3.3) are the same as those obtained by approximating the usual nonrelativistic two-body interaction potentials by hard core (delta) potentials, e.g.,

$$\int d^3x \Phi^*(\mathbf{x}, t)\Phi(\mathbf{x}, t)V_\Phi(\mathbf{x} - \mathbf{x}')\Phi^*(\mathbf{x}', t)\Phi(\mathbf{x}', t)$$
$$\rightarrow g_\Phi[\Phi^*(\mathbf{x}, t)\Phi(\mathbf{x}, t)]^2,$$
$$\int d^3x \Psi^*(\mathbf{x}, t)\Psi(\mathbf{x}, t)V_\Psi(\mathbf{x} - \mathbf{x}')\Psi^*(\mathbf{x}', t)\Psi(\mathbf{x}', t)$$
$$\rightarrow g_\Psi[\Psi^*(\mathbf{x}, t)\Psi(\mathbf{x}, t)]^2, \qquad (3.5)$$
$$\int d^3x \Phi^*(\mathbf{x}, t)\Phi(\mathbf{x}, t)V_{\Phi\Psi}(\mathbf{x} - \mathbf{x}')\Psi^*(\mathbf{x}', t)\Psi(\mathbf{x}', t)$$
$$\rightarrow g_{\Phi\Psi}[\Phi^*(\mathbf{x}, t)\Phi(\mathbf{x}, t)][\Psi^*(\mathbf{x}, t)\Psi(\mathbf{x}, t)].$$

The approximation of the two-body potential interactions like in (3.5) is also commonly adopted in the description of cold dilute atomic systems, where only binary type

interactions at low energy are relevant. In that case, the local coupling parameters g_Φ, g_Ψ and $g_{\Phi\Psi}$ are also associated to the s-wave scattering lengths a_i [9], e.g., $g_i = 2\pi a_i/m_i$. For nonrelativistic systems in general, besides the two-body interaction terms like (3.5) (in the hard core approximation) we can also include additional one-body like interaction terms, e.g., $\kappa_\Phi\Phi^*\Phi$, etc. This is the case when we submit the system to an external potential (for example a magnetic field). It can also represent an internal energy term (like the internal molecular energy relative to free atoms in which case the fields in the Lagrangian would be related to molecular dimers). In models of superconductivity a constant one-body like interaction term represents the opening of an explicit gap of energy in the system. In the grand-canonical formulation κ_i can represent chemical potentials included in the action formulation, so that one can also describe density effects (in addition to those from the temperature). In order to retain the symmetry breaking analogies to the previous relativistic model (2.1), and since our intention here is to keep the analysis as general as possible, we shall also consider additional one-body interaction terms for Φ and Ψ while their precise interpretation is left as open and will depend on the particular system Eq. (3.3) is intended to represent.

With the considerations assumed above, we therefore take the following nonrelativistic Lagrangian model, that is analogue to the relativistic model Eq. (2.1),

$$\mathcal{L}(\Phi^*, \Phi, \Psi^*, \Psi) = \Phi^*\left(i\partial_t + \frac{1}{2m_\Phi}\nabla^2\right)\Phi - \kappa_\Phi\Phi^*\Phi$$
$$- \frac{g_\phi}{3!}(\Phi^*\Phi)^2 + \Psi^*\left(i\partial_t + \frac{1}{2m_\Psi}\nabla^2\right)\Psi$$
$$- \kappa_\Psi\Psi^*\Psi - \frac{g_\psi}{3!}(\Psi^*\Psi)^2$$
$$- g(\Phi^*\Phi)(\Psi^*\Psi), \qquad (3.6)$$

---

[3]Note that for equal masses there is the possibility of an additional symmetric interaction term of the form $[(\Phi\Psi^*)^2 + (\Phi^*\Psi)^2]$ in (3.3), however this term will not be relevant for our analysis and conclusions since it can be absorbed in a redefinition of the cross-coupling constant λ, especially when we work with densities, or averages of the fields, like in an effective potential calculation.

where we have expressed the derivative terms in their more common form (by doing an integration by parts in the action context). The numerical factors and signs in the one and two-body potential terms in (3.6) have been chosen in such a way so that the potential in (3.6) are analogous to the one considered in (2.1). The coupling constants shown in (3.6) are related to those in (3.3) by $g_i = 3\lambda_i/(8m_i^2)$ (with $i = \Phi, \Psi$) and $g = \lambda/(4m_\Phi m_\Psi)$ while m_Φ and m_Ψ represent the (atomic) masses. In addition, notice that for the nonrelativistic limit which leads to Eq. (3.6) to be valid, one must keep $T \ll m_i$. Since for nonrelativistic systems in general, the masses m_i are of order of typical atomic masses, $m_i \sim \mathcal{O}(1\text{--}100)\text{GeV}$, and the typical temperatures in condensed matter systems are at most of order of a few eV, this condition will always hold for the ranges of temperature we will be interested in below.

For multicomponent fields, Eq. (3.6) is the nonrelativistic multiscalar model with symmetry $U(N_\Phi) \times U(N_\Psi)$ that is the analogue of the original relativistic model Eq. (2.1). For simplicity, in the following we assume the simplest version of (3.6) where $N_\Phi = N_\Psi = 1$, corresponding to an $U(1) \times U(1)$ symmetric model. In this case, by writing the complex fields in terms of real components,

$$\Phi = \frac{1}{\sqrt{2}}(\phi_1 + i\phi_2), \qquad \Psi = \frac{1}{\sqrt{2}}(\psi_1 + i\psi_2), \quad (3.7)$$

we see that the Lagrangian model (3.6) falls in the same class of universality as that of Eq. (2.1) for the case of the $O(2) \times O(2)$ symmetry. The extension to higher symmetries can be done starting from (3.6) but the case of simplest symmetry involving the coupling of complex scalar fields will already be sufficient for our study (physically, this system may, for example, describe the coupling of Bose atoms or molecules in an atomic dilute gas system).

Just like in the relativistic case, in the current application we consider the κ_i, that appears in Eq. (3.6), as simple temperature independent parameters for which thermal corrections arise from the evaluation of the corresponding field self-energies. Now, to make contact with the analogous potential used in the prototype relativistic models for SNR/ISB, we take the overall potential as being repulsive, bounded from below. This requirement imposes a constraint condition analogous to the one found in the relativistic case, $g_\Psi > 0$, $g_\Phi > 0$ and $g_\Psi g_\Phi > 9g^2$. At a given temperature, the phase structure of the model is then given by the sign of $\kappa_i(T) = \kappa_i + \Sigma_i$, where Σ_i is the field temperature dependent self-energy. In the broken phase $\kappa_i(T) < 0$, while in the symmetric phase $\kappa_i(T) > 0$. The phase transition occurs at $\kappa_i(T = T_c^i) = 0$. At the one-loop level the diagrams contributing to the field self-energies are the same as those in the relativistic case. The main difference is that the momentum integrals in the loops are now given in terms of the nonrelativistic propagators for Φ and Ψ,

$$D_i(\omega_n, \mathbf{q}) = \frac{1}{-i\omega_n + \omega_i(\mathbf{q})}, \quad (3.8)$$

where $\omega_n = 2\pi nT$ $(n = 0, \pm 1, \pm 2, \dots)$ are the bosonic Matsubara frequencies and $\omega_i(\mathbf{q}) = \mathbf{q}^2/(2m_i) + \kappa_i$. At the one-loop level we then obtain (see appendix)

$$\Sigma_i(T) = T \sum_{n=-\infty}^{+\infty} \int \frac{d^3q}{(2\pi)^3} \left[\frac{2g_i/3}{-i\omega_n + \omega_i(\mathbf{q})} + \frac{g}{-i\omega_n + \omega_j(\mathbf{q})} \right], \quad (3.9)$$

The sum in Eq. (3.9) can be easily performed and the resulting momentum integrals lead to well-known Bose integrals (see e.g. Ref. [24] and also the appendix for the derivations of these equations). We then obtain the results

$$\kappa_\Phi(T) = \kappa_\Phi + \frac{2g_\Phi}{3}\left(\frac{m_\Phi T}{2\pi}\right)^{3/2}\text{Li}_{3/2}[\exp(-\kappa_\Phi/T)] + g\left(\frac{m_\Psi T}{2\pi}\right)^{3/2}\text{Li}_{3/2}[\exp(-\kappa_\Psi/T)], \quad (3.10)$$

and

$$\kappa_\Psi(T) = \kappa_\Psi + \frac{2g_\Psi}{3}\left(\frac{m_\Psi T}{2\pi}\right)^{3/2}\text{Li}_{3/2}[\exp(-\kappa_\Psi/T)] + g\left(\frac{m_\Phi T}{2\pi}\right)^{3/2}\text{Li}_{3/2}[\exp(-\kappa_\Phi/T)], \quad (3.11)$$

where $\text{Li}_n(z_i)$ is the polylogarithmic function. Like in the relativistic effective mass terms, in Eqs. (3.10) and (3.11) we have once again limited to showing the temperature dependent corrections coming from Σ_i, omitting the divergent (zero-point energy terms) contributions to the effective one-body terms (so the tree-level parameters in Eqs. (3.10) and (3.11) are assumed to be already the renormalized ones). Let us now consider the high temperature approximation, which in the nonrelativistic case is valid as long as $\kappa_i \ll T \ll m_i$. Then, one is allowed to consider the approximation for the polylogarithmic functions in Eqs. (3.10) and (3.11), $\text{Li}_{3/2}[\exp(-\kappa_i/T)] \sim \zeta(3/2)$, where $\zeta(x)$ is the Riemann zeta function and $\zeta(3/2) \simeq 2.6124$. One can then write the two Eqs. (3.10) and (3.11) in the high temperature approximation more compactly, as

$$\kappa_i(T) \simeq \kappa_i + \left(\frac{T}{2\pi}\right)^{3/2}\zeta(3/2)\Delta_i^{\text{NR}}, \quad (3.12)$$

where we defined the quantity Δ_i^{NR} analogous to that of the relativistic case,

$$\Delta_i^{\text{NR}} = \frac{2}{3}g_i m_i^{3/2} + g m_j^{3/2}, \quad (3.13)$$

in terms of which we obtain the critical temperature for symmetry restoration/breaking analogous to the relativistic

expression,

$$T_{c,i}^{\mathrm{NR}} = 2\pi \left[\frac{-\kappa_i}{\Delta_i^{\mathrm{NR}} \zeta(3/2)} \right]^{2/3}. \qquad (3.14)$$

Equation (3.14) shows that there are three interesting cases which depend on the sign and magnitude of the cross-coupling g. Taking $\kappa_i < 0$ and $g > 0$ one observes a shift in the critical temperatures indicating that the transition occurs at lower temperatures compared to the decoupled case ($g = 0$). If $g < 0$ but $|g| < (2/3)g_i(m_i/m_j)^{3/2}$ then the transition occurs at higher temperatures. Despite these quantitative differences symmetry restoration does take place in both cases. Now consider for instance the case, with $\kappa_\Phi < 0$, where $g < 0$ but $|g| > (2/3)g_\Phi(m_\Phi/m_\Psi)^{3/2}$ (in this case, and assuming $m_\Phi \sim m_\Psi$, the boundness condition assures that $|g| < (2/3)g_\Psi$). Under these conditions, for the Φ field we have a similar situation as that for the corresponding relativistic case studied in Sec. II, where, Eq. (3.14) does not give a finite, positive real quantity. This is a manifestation of ISB (for $\kappa_\Phi < 0$, or SNR, for $\kappa_\Phi > 0$) within our two-field complex nonrelativistic model being analogous to what is seen in the relativistic case. At the same time the field Ψ suffers the expected phase transition at a higher T_c compared to the $g = 0$ case. As in the relativistic case, which field will suffer SNR/ISB depends on our initial choice of parameters in the tree-level potential, so it is model dependent. The SNR/ISB result as seen above in this nonrelativistic model is however misleading, as we next show by considering the same phenomenon in terms of the effective, temperature dependent, coupling parameters.

Physically, the possibility of SNR/ISB occurring at high temperatures as predicted by the naive perturbative approximation, Eq. (3.12), is much harder to be accepted in the nonrelativistic case (condensed matter) than in the relativistic case (cosmology), which already seems to indicate that the results here should be different when the simple perturbative calculations are improved.

Following the analogy with the relativistic model calculation done in Sec. II, we next evaluate the temperature effects on the nonrelativistic couplings.

The diagrams contributing to the effective self-couplings $g_\Phi(T)$ and $g_\Psi(T)$, at the one-loop level, are those shown in Figs. 1 and 2, respectively, except that the s-channel ones with internal propagators for fields different from those in the external legs (the second one-loop diagrams in Figs. 1 and 2 made of vertices nonconserving particles) are absent. For the effective cross-coupling $g(T)$, as discussed at the beginning of this section, the diagrams contributing at the one-loop level are the ones shown in Fig. 3(a), corresponding to the particle number preserving processes. Using (3.8) for the nonrelativistic field propagators, the explicit expressions for the effective couplings at one-loop order are found to be (see also the appendix)

$$g_\Phi(T) = g_\Phi - \frac{g_\Phi^2}{3} \int \frac{d^3\mathbf{q}}{(2\pi)^3} \frac{1}{2\omega_\Phi(\mathbf{q})} \{1 + 2n(\omega_\Phi) + 8\beta\omega_\Phi n(\omega_\Phi)[1 + n(\omega_\Phi)]\} - 3g^2 \int \frac{d^3\mathbf{q}}{(2\pi)^3} \beta n(\omega_\Psi)[1 + n(\omega_\Psi)], \qquad (3.15)$$

$$g_\Psi(T) = g_\Psi - \frac{g_\Psi^2}{3} \int \frac{d^3\mathbf{q}}{(2\pi)^3} \frac{1}{2\omega_\Psi(\mathbf{q})} \{1 + 2n(\omega_\Psi) + 8\beta\omega_\Psi n(\omega_\Psi)[1 + n(\omega_\Psi)]\} - 3g^2 \int \frac{d^3\mathbf{q}}{(2\pi)^3} \beta n(\omega_\Phi)[1 + n(\omega_\Phi)], \qquad (3.16)$$

and

$$g(T) = g - \frac{2g}{3} \int \frac{d^3\mathbf{q}}{(2\pi)^3} \beta \{g_\Phi n(\omega_\Phi)[1 + n(\omega_\Phi)] + g_\Psi n(\omega_\Psi)[1 + n(\omega_\Psi)]\} - g^2 \int \frac{d^3\mathbf{q}}{(2\pi)^3} \{\frac{\omega_\Psi}{\omega_\Psi^2 - \omega_\Phi^2}[1 + 2n(\omega_\Phi)] - \frac{\omega_\Phi}{\omega_\Psi^2 - \omega_\Phi^2}[1 + 2n(\omega_\Psi)]\}. \qquad (3.17)$$

The numerical factors in Eqs. (3.15), (3.16), and (3.17) are due to the symmetries of the diagrams and normalizations chosen in Eq. (3.6). In the above equations, $n(\omega)$ is the Bose-Einstein distribution

The zero temperature contributions in Eqs. (3.15), (3.16), and (3.17) are divergent and require proper renormalization. This is mostly simply done by performing the momentum integrals in $d = 3 - \epsilon$ dimensions and the resulting integrals are all found to be finite in dimensional regularization (when taking $\epsilon \to 0$ at the end). The momentum integrals for the finite temperature contributions in Eqs. (3.15), (3.16), and (3.17) can again be performed with the help of the Bose integrals given in the appendix. We can further simplify the equations by considering parameters such as $m_\Phi \simeq m_\Psi = m$, $\kappa_\Phi \simeq \kappa_\Psi = \kappa$ and temperatures satisfying $\kappa \ll T \ll m$ in which case the zero temperature corrections to the couplings are negligible compared to the finite temperature ones and can safely be neglected. At leading order, in T, we then obtain the results

$$g_\Phi(T) \simeq g_\Phi - \frac{mT}{12\pi} \sqrt{\frac{2m}{\kappa}} (5g_\Phi^2 + 9g^2) + \mathcal{O}(\kappa/T), \quad (3.18)$$

$$g_\Psi(T) \simeq g_\Psi - \frac{mT}{12\pi} \sqrt{\frac{2m}{\kappa}} (5g_\Psi^2 + 9g^2) + \mathcal{O}(\kappa/T), \quad (3.19)$$

and

$$g(T) \simeq g - \frac{mT}{4\pi} \sqrt{\frac{2m}{\kappa}} g(g + \frac{2g_\Phi}{3} + \frac{2g_\Psi}{3}) + \mathcal{O}(\kappa/T).$$
$$(3.20)$$

Note from Eqs. (3.18), (3.19), and (3.20) that the effective couplings in the nonrelativistic theory have a much stronger dependence with the temperature than in those in the equivalent relativistic theory, Eqs. (2.9), (2.10), and (2.11). We therefore expect to see larger deviations at high temperatures for the effective couplings as compared with the same case in the relativistic problem (by high temperature we mean here temperatures larger than the typical one-body potential coefficients in (3.6), but much less than the particle masses, see above). It is also evident from the analysis of higher loop corrections to the effective couplings in the nonrelativistic model that all bubble-like corrections contribute with the same power in temperature as the one-loop terms, which can easily be checked by simple power-counting in the momentum. A side effect of this is the breakdown, at high temperatures, of the simple one-loop perturbation theory applied here. Another symptom is the apparent running of the effective self-couplings,

shown above, to negative values for sufficiently high temperatures given by $T \gtrsim T_{\text{break}} \sim \min(12\pi\sqrt{\kappa/(2m^{3/2})}g_\Phi/(5g_\Phi^2 + 9g^2), 12\pi\sqrt{\kappa/(2m^{3/2})}g_\Psi/(5g_\Psi^2 + 9g^2))$. Nevertheless, it is easy to check that (for the parameters adopted below) the results obtained by just plugging Eqs. (3.18), (3.19), and (3.20) above into Eqs. (3.12) already show a drastic qualitative difference between this simple improved approximation and the naive perturbative evaluation given by Eq. (3.12). It looks that for the nonrelativistic case SNR/ISB is a mere artifact of perturbation theory. Intuitively, this is already a rather satisfactory result which, as we will show below, will be confirmed by a nonperturbative resummation of the bubble-like corrections. The resumming of all leading order bubble corrections to the couplings can again be done by solving the set of homogeneous linear equations for $g_\Phi(T)$, $g_\Psi(T)$ and $g(T)$,

$$g_\Phi(T) = g_\Phi - g_\Phi(T)\frac{g_\Phi}{3}I_1(\beta\kappa_\Phi) - 3g(T)gI_2(\beta\kappa_\Psi), \qquad g_\Psi(T) = g_\Psi - g_\Psi(T)\frac{g_\Psi}{3}I_1(\beta\kappa_\Psi) - 3g(T)gI_2(\beta\kappa_\Phi),$$

$$g(T) = g - g(T)\frac{2g_\Phi}{6}I_2(\beta\kappa_\Phi) - g(T)\frac{2g_\Psi}{6}I_2(\beta\kappa_\Psi)g_\Phi(T)\frac{2g}{6}I_2(\beta\kappa_\Phi) - g_\Psi(T)\frac{2g}{6}I_2(\beta\kappa_\Psi) - g(T)gI_3(\beta\kappa_\Phi, \beta\kappa_\Psi),$$

$$(3.21)$$

where we have defined the functions

$$I_1(\beta\kappa_i) = \int \frac{d^3\mathbf{q}}{(2\pi)^3}\frac{1}{2\omega_i(\mathbf{q})}\{1 + 2n(\omega_i) + 8\beta\omega_i n(\omega_i)[1 + n(\omega_i)]\}, \qquad I_2(\beta\kappa_i) = \int \frac{d^3\mathbf{q}}{(2\pi)^3}\beta n(\omega_i)[1 + n(\omega_i)],$$

$$I_3(\beta\kappa_i, \beta\kappa_j) = \int \frac{d^3\mathbf{q}}{(2\pi)^3}\left\{\frac{\omega_j}{\omega_j^2 - \omega_i^2}[1 + 2n(\omega_i)] - \frac{\omega_i}{\omega_j^2 - \omega_i^2}[1 + 2n(\omega_j)]\right\}.$$

$$(3.22)$$

One is now in position to investigate how thermal effects on the effective nonrelativistic couplings manifest themselves in phenomena similar to SNR/ISB. First we show in Fig. 7 some representative results for the effective inter-
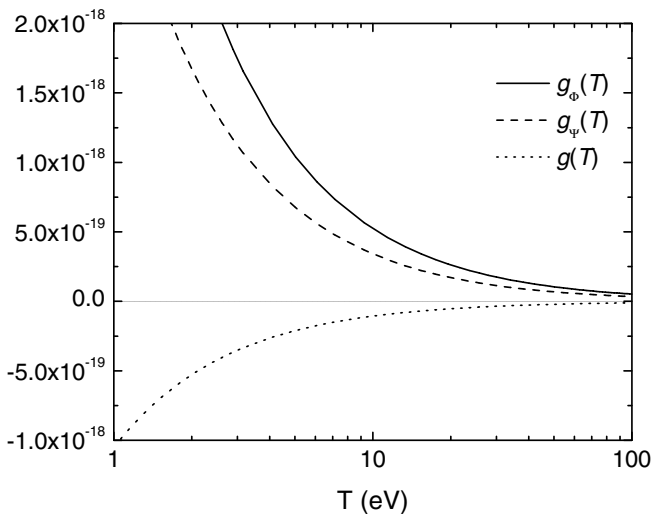

FIG. 7.   The nonrelativistic effective couplings as a function of temperature (shown in units of eV).

actions obtained from the solutions of Eq. (3.21). The tree-level parameters considered here are: $g_\Phi = 2 \times 10^{-15}$ eV^{-2}, $g_\Psi = 10^{-16}$ eV^{-2}, $g = -10^{-16}$ eV^{-2}, $m_\Phi \simeq m_\Psi = 1$ GeV and $\kappa_\Phi = \kappa_\Psi = 1$ neV. We note that all couplings tend to evolve to zero at very high temperatures as T gets closer to m. So, the apparent instability caused by the fact that $g_\Psi(T)$ as well as $g_\Phi(T)$ could become negative beyond some temperature, T_{break}, as suggested by Eqs. (3.18) and (3.19), has disappeared completely when the nonperturbative flow of the couplings are considered (using the tree-level parameters given above and from Eqs. (3.18) and (3.19), one would get $T_{\text{break}} \sim 0.019$ eV (or $\sim 220K$).

It is tempting, by looking at Fig. 7, to associate this to a free model at high energies, however we must recall that the nonrelativistic model, Eq. (3.6), will eventually no longer be valid for such high values of temperature, in which case it should be replaced by the original relativistic model (in any case the model Eq. (3.6) should of course be regarded as an effective model valid at low-energy scales only).

In Fig. 8 we show the equivalent of Eq. (3.13) for the Φ and Ψ fields, $\Delta_\Phi^{\text{NR}}(T)$ and $\Delta_\Psi^{\text{NR}}(T)$, respectively, given in terms of the temperature dependent bubble resummed

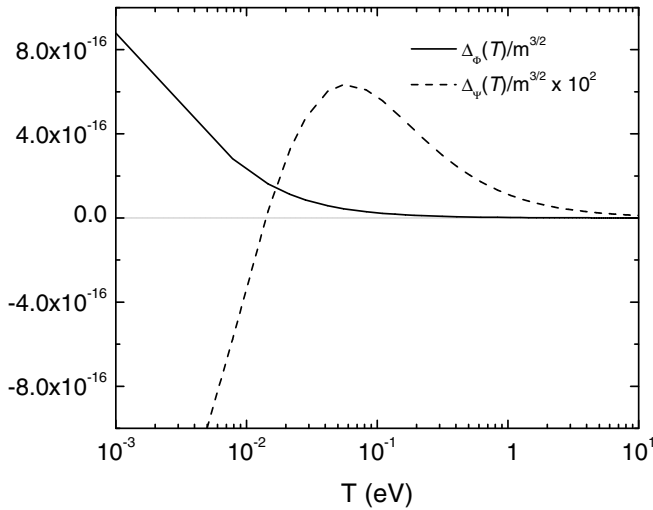FIG. 8.   The quantities $\Delta_\Phi^{NR}(T)/m^{3/2}$ and $\Delta_\Psi^{NR}(T)/m^{3/2}$ as a function of the temperature for the same values of parameters used in Fig. 7.

couplings for the same tree-level parameters considered above. We note that for the parameters considered $\Delta_\Psi^{NR}(T)$ is initially negative and reverse sign at some temperature, indicating that symmetry breaking at high temperatures tends to happen in the Ψ field direction, while the potential in the Φ direction remains unbroken (actually, the temperature where $\Delta_\Psi^{NR}(T)$ crosses zero, is close to the point of a reentrant transition for Ψ). $\Delta_\Phi^{NR}(T)$ however always remains positive, which then points to no transition in the Φ direction. These aspects are also clearly seen in the plot, shown in Fig. 9, for the effective one-body term $\kappa_\Psi(T)$, expressed in terms of the effective nonperturbative cou-
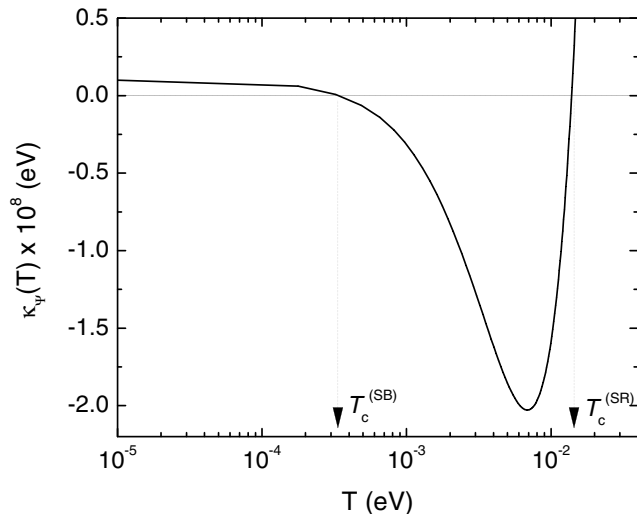

FIG. 9.   The nonperturbative effective one-body term $\kappa_\Psi(T)$ as a function of the temperature for the same values of parameters used in Fig. 7. Both quantities are expressed in units of eV. The arrows indicate the points of SB and SR, with an intermediary ISB phase happening between the temperatures $T_c^{SB} < T < T_c^{SR}$.
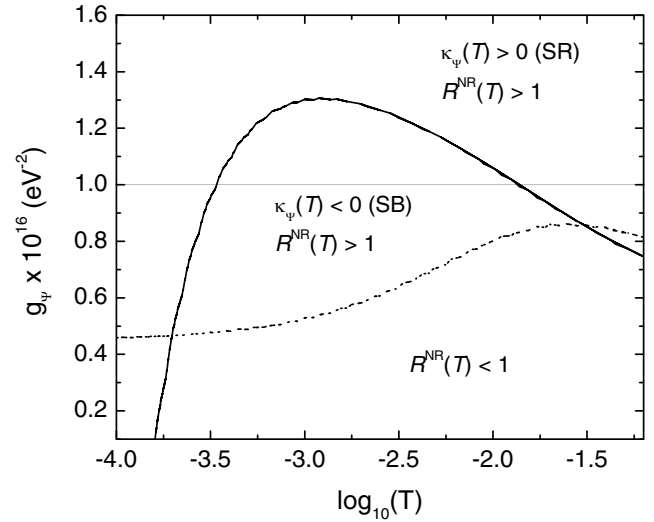

FIG. 10.   A phase diagram of the system for fixed parameters: $g_\Phi = 2 \times 10^{-15}$ eV^{-2}, $g = -10^{-16}$ eV^{-2}, $m_\Phi \simeq m_\Psi = 1$ GeV and $\kappa_\Phi = \kappa_\Psi = 1$ neV. The dotted line separates the region of stability ($R^{NR}(T) > 1$) from that of instability ($R^{NR}(T) < 1$), according to the value of the ratio $R^{NR}(T) = g_\Psi(T)g_\Phi(T)/[9g^2(T)]$. The regions of SR and SB, in the Ψ direction, are also shown. The thin horizontal line indicates the value of g_Ψ used in the text.

plings. In terms of the parameters considered, symmetry breaking is seen to happen at a temperature $T_{c,\Psi}^{(SB)} \simeq 3.4 \times 10^{-4}$eV (or ~4K) while the reentrant phase (symmetry restoration) happens at a temperature $T_{c,\Psi}^{(SR)} \simeq 1.4 \times 10^{-2}$ eV (or ~161K). In between these two temperatures we see a manifestation of an ISB phase. In the Φ direction there is no symmetry breaking or reentrant phases at any temperature for the parameters considered.

In Fig. 10 we show a phase diagram for the system as a function of the tree-level coupling g_Ψ and the temperature. The thin horizontal line at $g_\Psi = 10^{-16}$eV^{-2} illustrates the reentrant transition (through an inverse symmetry breaking) shown in Fig. 9. All other parameters are the same as considered above. Note that the condition of stability, $g_\Psi g_\Phi > 9g^2$, expressed in terms of the nonperturbative and temperature dependent couplings, is always satisfied at any temperature for the parameters considered for the previous figures (the effective couplings g_Ψ and g_Φ also remain always positive, as is clear from Fig. 7 and previous discussion).

IV. CONCLUSIONS

We have reviewed how symmetry nonrestoration and inverse symmetry breaking may take place, at arbitrarily large temperatures, in multifield scalar relativistic and nonrelativistic theories. These counterintuitive phenomena appear due to the fact that the crossed interaction can be negative while the models are still bounded from below. We have recalled that, in the relativistic case, SNR/ISB are

not a mere artifact of calculational approximations. We have then set to investigate the possible SNR/ISB manifestation and consequences in a nonrelativistic $U(N_\Phi) \times U(N_\Psi)$ scalar model of hard core spheres by considering the simplest case, $N_\Phi = N_\Psi = 1$, which may be relevant for condensed matter systems of bosonic atoms or molecules.

Performing a naive perturbative one-loop calculation, which includes only the first thermal contribution to the self-energy, we have shown that, for negative values of the crossed coupling, SNR/ISB can take place like in the relativistic case. However, the manifestation of SNR/ISB in condensed matter systems of hard core spheres seems to be more counterintuitive than in the relativistic case where the model may represent, e.g., the Higgs sector. With this in mind we have investigated the explicit (temperature) running of the nonrelativistic couplings. One first improvement was to evaluate the perturbative one-loop thermal corrections to the couplings which already indicate that SNR/ISB do not seem to happen, at high temperatures, for the nonrelativistic case. Next, we have resummed the bubble-like contributions in a nonperturbative fashion. This procedure fixed the instability problem related to the possibility of $g_i(T)$ becoming negative as observed in the calculation which considered only the simplest one-loop corrections to the couplings. Our nonperturbative calculation also showed that the phase transitions happening in the nonrelativistic case includes a continuous SB/SR pattern characterized, at intermediate temperatures, by a reentrant, continuous transition. Therefore, we can state as our major result that, contrary to the relativistic case, SNR/ISB does not seem to occur in the nonrelativistic model of hard core spheres. Instead, reentrant like phenomena become possible, as our results have indicated.

Finally, it would be interesting to investigate SNR/ISB in connection with the Bose-Einstein condensation problem and the present work gives some of the ideas and tools needed for this task that we hope to pursue and report in a future publication.

ACKNOWLEDGMENTS

APPENDIX: TEMPERATURE DEPENDENT CORRECTIONS FOR THE NONRELATIVISTIC MODEL

Here we give the main steps used in the evaluation of the thermal masses and couplings for the nonrelativistic model. Similar derivations for the relativistic model can be found e.g. in Refs. [3,4,18].

The effective one-body terms $\kappa_i(T)$ and the effective couplings (two-body terms) for the nonrelativistic model are most easily obtained directly from a computation of the one-loop effective potential for the model Lagrangian (3.6). The effective one and two-body terms will then be identified with the appropriate derivatives of the effective potential.

As usual in the computation of the one-loop potential, we start by decomposing the fields Φ and Ψ in (3.6) in terms of (constant) background fields (which, without loss of generality, can be taken as real fields) ϕ_0 and ψ_0, respectively, and fluctuations ϕ and ψ, which in terms of real components, become

$$\Phi = \frac{1}{\sqrt{2}}(\phi_0 + \phi_1 + i\phi_2), \tag{A1}$$

$$\Psi = \frac{1}{\sqrt{2}}(\psi_0 + \psi_1 + i\psi_2). \tag{A2}$$

When substituting Eqs. (A1) and (A2) in (3.6) we only need keep the quadratic terms in the fluctuation fields for the computation of the one-loop potential for the background fields ϕ_0 and ψ_0. We then obtain the (Euclidean) Lagrangian density in terms of ϕ_0 and ψ_0,

$$\mathcal{L}_E = \frac{\kappa_\Phi}{2}\phi_0^2 + \frac{g_\Phi}{4!}\phi_0^4 + \frac{\kappa_\Psi}{2}\psi_0^2 + \frac{g_\Psi}{4!}\psi_0^4 + \frac{g}{4}\phi_0^2\psi_0^2$$
$$+ \frac{1}{2}\chi \cdot \hat{M} \cdot \chi + \text{cubic and quartic interaction terms,} \tag{A3}$$

where we have defined the vector $\chi = (\phi_1, \phi_2, \psi_1, \psi_2)$ and $\hat{M}$ is the matrix operator for the quadratic terms in the fluctuations,

$$\hat{M} = \begin{pmatrix} \frac{-\nabla^2}{2m_\Phi} + \kappa_\Phi + \frac{g_\Phi}{2}\phi_0^2 + \frac{g}{2}\psi_0^2 & i\partial_\tau & g\phi_0\psi_0 & 0 \\ -i\partial_\tau & \frac{-\nabla^2}{2m_\Phi} + \kappa_\Phi + \frac{g_\Phi}{6}\phi_0^2 + \frac{g}{2}\psi_0^2 & 0 & 0 \\ g\phi_0\psi_0 & 0 & \frac{-\nabla^2}{2m_\Psi} + \kappa_\Psi + \frac{g_\Psi}{2}\psi_0^2 + \frac{g}{2}\phi_0^2 & i\partial_\tau \\ 0 & 0 & -i\partial_\tau & \frac{-\nabla^2}{2m_\Psi} + \kappa_\Psi + \frac{g_\Psi}{6}\psi_0^2 + \frac{g}{2}\phi_0^2 \end{pmatrix}. \tag{A4}$$

The partial time derivative in (A4) is over Euclidean time: $\partial_\tau = \partial/\partial\tau$, $\tau = it$. By performing the functional integration in the quadratic fluctuations χ, the one-loop effective potential $V_{\text{eff}}(\phi_0, \psi_0)$ obtained from Eq. (A3) is given by

$$V_{\text{eff}}(\phi_0, \psi_0) = \frac{\kappa_\Phi}{2}\phi_0^2 + \frac{g_\Phi}{4!}\phi_0^4 + \frac{\kappa_\Psi}{2}\psi_0^2 + \frac{g_\Psi}{4!}\psi_0^4$$
$$+ \frac{g}{4}\phi_0^2\psi_0^2 + \frac{1}{2}\ln\det\hat{M}, \tag{A5}$$

where the last term on the right-hand side of (A5) comes from the functional integral over the components of χ,

$$\frac{1}{2}\ln\det\hat{M} = -\frac{1}{\beta V}\int D\phi_1 D\phi_2 D\psi_1 D\psi_2$$
$$\times \exp\left[-\int_0^\beta d\tau \int d^3x\left(\frac{1}{2}\chi\cdot\hat{M}\cdot\chi\right)\right], \tag{A6}$$

and V is the volume of space. Expressing Eqs. (A6) and (A4) in the space-time momentum Fourier transform form, we then also obtain

$$\frac{1}{2}\ln\det\hat{M} = \frac{1}{2}\frac{1}{\beta}\sum_n \int \frac{d^3\mathbf{q}}{(2\pi)^3}\ln\{[\omega_n^2 + E_\Phi^2(\mathbf{q})]$$
$$\times[\omega_n^2 + E_\Psi^2(\mathbf{q})] - g^2\phi_0^2\psi_0^2\}, \tag{A7}$$

with

$$E_\Phi(\mathbf{q}) = \sqrt{\left[\omega_\Phi(\mathbf{q}) + \frac{g_\Phi}{2}\phi_0^2 + \frac{g}{2}\psi_0^2\right]\left[\omega_\Phi(\mathbf{q}) + \frac{g_\Phi}{6}\phi_0^2 + \frac{g}{2}\psi_0^2\right]}, \tag{A8}$$

and

$$E_\Psi(\mathbf{q}) = \sqrt{\left[\omega_\Psi(\mathbf{q}) + \frac{g_\Psi}{2}\psi_0^2 + \frac{g}{2}\phi_0^2\right]\left[\omega_\Psi(\mathbf{q}) + \frac{g_\Psi}{6}\psi_0^2 + \frac{g}{2}\phi_0^2\right]}. \tag{A9}$$

From $V_{\text{eff}}(\phi_0, \psi_0)$, Eq. (A5), we now define the effective one-body terms as

$$\kappa_\Phi(T) = \frac{\partial^2 V_{\text{eff}}(\phi_0, \psi_0)}{\partial\phi_0^2}\bigg|_{\phi_0=0,\psi_0=0}, \tag{A10}$$

$$\kappa_\Psi(T) = \frac{\partial^2 V_{\text{eff}}(\phi_0, \psi_0)}{\partial\psi_0^2}\bigg|_{\phi_0=0,\psi_0=0}, \tag{A11}$$

which then gives

$$\kappa_\Phi(T) = \kappa_\Phi + \frac{2g_\Phi}{3}\frac{1}{\beta}\sum_n \int \frac{d^3\mathbf{q}}{(2\pi)^3}\frac{\omega_\Phi(\mathbf{q})}{\omega_n^2 + \omega_\Phi^2(\mathbf{q})}$$
$$+ g\frac{1}{\beta}\sum_n \int \frac{d^3\mathbf{q}}{(2\pi)^3}\frac{\omega_\Psi(\mathbf{q})}{\omega_n^2 + \omega_\Psi^2(\mathbf{q})}, \tag{A12}$$

and

$$\kappa_\Psi(T) = \kappa_\Psi + \frac{2g_\Psi}{3}\frac{1}{\beta}\sum_n \int \frac{d^3\mathbf{q}}{(2\pi)^3}\frac{\omega_\Psi(\mathbf{q})}{\omega_n^2 + \omega_\Psi^2(\mathbf{q})}$$
$$+ g\frac{1}{\beta}\sum_n \int \frac{d^3\mathbf{q}}{(2\pi)^3}\frac{\omega_\Phi(\mathbf{q})}{\omega_n^2 + \omega_\Phi^2(\mathbf{q})}, \tag{A13}$$

The Eqs. (A12) and (A13) can also easily be expressed in terms of the free nonrelativistic propagators $D_\Phi(\omega_n, \mathbf{q})$ and $D_\Psi(\omega_n, \mathbf{q})$. The sum over the Matsubara frequencies in (A12) and (A13) are easily performed by using the identity [17],

$$\frac{1}{\beta}\sum_n \frac{1}{\omega_n^2 + \omega^2} = \frac{1}{\omega}\left[\frac{1}{2} + n(\omega)\right], \tag{A14}$$

where $n(\omega)$ is the Bose-Einstein distribution,

$$n(\omega) = \frac{1}{e^{\beta\omega} - 1}. \tag{A15}$$

The momentum integrals in Eqs. (A12) and (A13) can be expressed in terms of standard Bose integrals as follows (see for example [24]). Consider the integral (where $\omega = \mathbf{q}^2/(2m) + \kappa$ and $\eta = \beta\kappa$)

$$\int \frac{d^3q}{(2\pi)^3}n(\omega) = \frac{1}{2\pi^2}\left(\frac{2m}{\beta}\right)^{3/2}\int_0^\infty dx\frac{x^2}{e^{x^2+\eta}-1}$$
$$= \frac{1}{2\pi^2}\left(\frac{2m}{\beta}\right)^{3/2}\sum_{l=1}^\infty e^{-l\eta}\int_0^\infty dxx^2e^{-lx^2}$$
$$= \left(\frac{m}{2\pi\beta}\right)^{3/2}\text{Li}_{3/2}(e^{-\beta\kappa}), \tag{A16}$$

where we used the definition for the polylogarithmic function,

$$\text{Li}_\alpha(z) = \sum_{l=1}^\infty \frac{z^l}{l^\alpha}. \tag{A17}$$

Another useful momentum integral that also can be obtained from (A16) is

$$\int \frac{d^3q}{(2\pi)^3}n(\omega)[1 + n(\omega)] = \left(\frac{m}{2\pi\beta}\right)^{3/2}\text{Li}_{1/2}(e^{-\beta\kappa}). \tag{A18}$$

We also have the results obtained from the polylogarithmic functions in the high temperature approximation, $\kappa \ll T$, and that are used in the text,

$$\text{Li}_{3/2}(e^{-\beta\kappa}) = \zeta(3/2) - 2\sqrt{\pi\frac{\kappa}{T}} + \mathcal{O}(\kappa/T), \tag{A19}$$

and

$$\text{Li}_{1/2}(e^{-\beta\kappa}) = \sqrt{\pi \frac{T}{\kappa}} - \zeta(1/2) + \mathcal{O}(\kappa/T). \qquad (A20)$$

Using (A16) in Eqs. (A12) and (A13) we obtain the results quoted in the text, Eqs. (3.10) and (3.11).

The two-body effective terms are also defined analogously as

$$g_\Phi(T) = \frac{\partial^4 V_{\text{eff}}(\phi_0, \psi_0)}{\partial \phi_0^4} \bigg|_{\phi_0=0, \psi_0=0}, \qquad (A21)$$

$$g_\Psi(T) = \frac{\partial^4 V_{\text{eff}}(\phi_0, \psi_0)}{\partial \psi_0^4} \bigg|_{\phi_0=0, \psi_0=0}, \qquad (A22)$$

and

$$g(T) = \frac{\partial^4 V_{\text{eff}}(\phi_0, \psi_0)}{\partial \phi_0^2 \partial \psi_0^2} \bigg|_{\phi_0=0, \psi_0=0}. \qquad (A23)$$

From Eqs. (A5) and (A7) we then obtain for Eqs. (A21)–(A23) the results

$$g_\Phi(T) = g_\Phi + \frac{1}{\beta} \sum_n \int \frac{d^3\mathbf{q}}{(2\pi)^3} \bigg\{ g_\Phi^2 \frac{1}{\omega_n^2 + \omega_\Phi^2(\mathbf{q})}$$
$$- \frac{8}{3} g_\Phi^2 \frac{\omega_\Phi^2(\mathbf{q})}{[\omega_n^2 + \omega_\Phi^2(\mathbf{q})]^2} + 3g^2 \frac{1}{\omega_n^2 + \omega_\Psi^2(\mathbf{q})}$$
$$- 6g^2 \frac{\omega_\Psi^2(\mathbf{q})}{[\omega_n^2 + \omega_\Psi^2(\mathbf{q})]^2} \bigg\}, \qquad (A24)$$

$$g_\Psi(T) = g_\Psi + \frac{1}{\beta} \sum_n \int \frac{d^3\mathbf{q}}{(2\pi)^3} \bigg\{ g_\Psi^2 \frac{1}{\omega_n^2 + \omega_\Psi^2(\mathbf{q})}$$
$$- \frac{8}{3} g_\Psi^2 \frac{\omega_\Psi^2(\mathbf{q})}{[\omega_n^2 + \omega_\Psi^2(\mathbf{q})]^2} + 3g^2 \frac{1}{\omega_n^2 + \omega_\Phi^2(\mathbf{q})}$$
$$- 6g^2 \frac{\omega_\Phi^2(\mathbf{q})}{[\omega_n^2 + \omega_\Phi^2(\mathbf{q})]^2} \bigg\}, \qquad (A25)$$

and

$$g(T) = g + \frac{1}{\beta} \sum_n \int \frac{d^3\mathbf{q}}{(2\pi)^3} \bigg\{ \frac{2}{3} g g_\Phi \frac{1}{\omega_n^2 + \omega_\Phi^2(\mathbf{q})}$$
$$- \frac{4}{3} g g_\Phi \frac{\omega_\Phi^2(\mathbf{q})}{[\omega_n^2 + \omega_\Phi^2(\mathbf{q})]^2} + \frac{2}{3} g g_\Psi \frac{1}{\omega_n^2 + \omega_\Psi^2(\mathbf{q})}$$
$$- \frac{4}{3} g g_\Psi \frac{\omega_\Psi^2(\mathbf{q})}{[\omega_n^2 + \omega_\Psi^2(\mathbf{q})]^2}$$
$$- 2g^2 \frac{\omega_\Phi(\mathbf{q})\omega_\Psi(\mathbf{q})}{[\omega_n^2 + \omega_\Phi^2(\mathbf{q})][\omega_n^2 + \omega_\Psi^2(\mathbf{q})]} \bigg\}. \qquad (A26)$$

The Eqs. (A24)–(A26) again can be expressed in terms of the free nonrelativistic propagators $D_\Phi(\omega_n, \mathbf{q})$ and $D_\Psi(\omega_n, \mathbf{q})$, which can then be identified with the corresponding one-loop diagrams that contribute here, depicted in Figs. 1, 2, and 3(a). All sums over the Matsubara frequencies in (A24)–(A26) are again evaluated with the help of the identity (A14), from which we obtain the results shown in Eqs. (3.15), (3.16), and (3.17).

[1] S. Weinberg, Phys. Rev. D **9**, 3357 (1974).
[2] B. Bajc, hep-ph/0002187.
[3] T. G. Roos, Phys. Rev. D **54**, 2944 (1996).
[4] M. B. Pinto and R. O. Ramos, Phys. Rev. D **61**, 125016 (2000).
[5] R. N. Mohapatra and G. Senjanović, Phys. Rev. Lett. **64**, 340 (1990); S. Dodelsons, B. R. Greene, and L. M. Widrow, Nucl. Phys. **B372**, 467 (1992).
[6] B. Bajc, A. Melfo, and G. Senjanović, Phys. Lett. B **387**, 796 (1996); A. Riotto and G. Senjanović, Phys. Rev. Lett. **79**, 349 (1997).
[7] G. Bimonte and G. Lozano, Phys. Lett. B **366**, 248 (1996); Nucl. Phys. **B460**, 155 (1996).
[8] R. N. Mohapatra and G. Senjanović, Phys. Rev. Lett. **42**, 1651 (1979); Phys. Rev. D **20**, 3390 (1979).
[9] Ph. W. Courteille, V. S. Bagnato, and V. I. Yukalov, Laser Phys. **11**, 659 (2001); F. Dalfovo, S. Giorgini, L. P. Pitaevskii, and S. Stringari, Rev. Mod. Phys. **71**, 463 (1999).
[10] F. Jona and G. Shirane, *Ferroelectric Crystals* (Pergamon, Oxford, 1962).
[11] P. Mach, *et al.*, Phys. Rev. Lett. **81**, 1015 (1998);

D. Pociecha, *et al.* Phys. Rev. Lett. **86**, 3048 (2001).
[12] Y. Taguchi, *et al.* Science **291**, 2573 (2001).
[13] S. Mori, *et al.*, Nature (London) **392**, 473 (1998); P. Dai, *et al.*, Phys. Rev. Lett. **85**, 2553 (2000).
[14] G. Schmid, *et al.*, Phys. Rev. Lett. **88**, 167208 (2002).
[15] N. Schupper and N. M. Shnerb, cond-mat/0502033.
[16] R. J. Rivers, in: *Proceedings of the National Workshop on Cosmological Phase Transitions and Topological Defects, Porto, Portugal, 2003*, edited by T. A. Girard (Grafitese, Edificio Ciencia, 2004), p. 11.
[17] L. Dolan and R. Jackiw, Phys. Rev. D **9**, 2904 (1974).
[18] P. Fendley, Phys. Lett. B **196**, 175 (1987).
[19] O. Bergman, Phys. Rev. D **46**, 5474 (1992).
[20] G. D. Mahan, *Many-particle Physics* (Plenum, New York, 1981).
[21] L. P. Kadanoff and G. Baym, *Quantum Statistical Mechanics* (Addison-Wesley, New York, 1989).
[22] R. L. Davis, Mod. Phys. Lett. A **5**, 955 (1990).
[23] A. Zee, *Quantum Field Theory in a Nut Shell* (Princeton University Press, Princeton, 2003).
[24] R. K. Pathria, *Statistical Mechanics* (Pergamon Press, Oxford, 1972).